ELSEVIER

Journal of Microbiological Methods 37 (1999) 201–213

Journal of Microbiological Methods

In situ imaging of microorganisms in geologic material

K.J. Tobin[a,*], T.C. Onstott[a], M.F. DeFlaun[b], F.S. Colwell[c], J. Fredrickson[d]

[a]*Department of Geosciences, Princeton University, Princeton, NJ 08544, USA*
[b]*Envirogen, Inc., Princeton Research Center, 4100 Quakerbridge Rd., Lawrenceville, NJ 08648, USA*
[c]*Biotechnologies Department, Idaho National Engineering and Environmental Laboratory, Idaho Falls, ID 83415, USA*
[d]*Pacific Northwest National Laboratories, Richland, WA 99352, USA*

Received 20 November 1998; received in revised form 19 February 1999; accepted 19 February 1999

Abstract

In order to fully delineate the interactions of microorganisms with geological substrates, unequivocal identification of intact microbial cells within geologic samples is required without the disruption of either the rock texture or the relationship of the microorganisms to the mineral fabric. To achieve this objective we developed a protocol that enables the visualization of intact microbial cells in petrographic thin sections, avoids detaching the cells from their host mineral surfaces and avoids microbial contamination during the lapidary process. Propidium iodide and POPO-3, nucleic acid stains that specifically target double-stranded DNA and RNA were utilized for in situ visualization of cells in surface and subsurface basalts from northeastern Idaho. Additionally, examination of samples incubated with acetic acid–UL–^{14}C via phosphor imagining facilitated the in situ visualization of ^{14}C labeled biomass. Biomass observed was low ($< 10^7$ cells/g). These observations indicate that the microbial distribution in these rocks exhibits a high degree of spatial heterogeneity at the sub-centimeter scale.

Keywords: Propidium iodide; Phosphor imaging; Petrographic thin section

1. Introduction

Several studies have demonstrated that subsurface microbial communities unequivocally impact ground water chemistry (e.g. Stevens and McKinley, 1995; Lovley et al., 1990). Subsurface microbial activity can potentially affect the mineralogy of the aquifer strata by facilitating dissolution and precipitation reactions (e.g. Hiebert and Bennett, 1992). The diagenetic features observed in subsurface samples may be due, at least in part, to ongoing microbial processes. Alternatively, they may be the result of geologically ancient alteration. Incontrovertible geochemical proof of the former is difficult to establish. Although intact, viable microbial cells have been recovered from subsurface rock samples, conventional enumeration procedures involve removal of the cells from their mineralogical host and textural context prior to quantification (e.g. Kepner and Pratt, 1993). Assessing the geochemical impact of subsurface microbial communities requires in situ identification of living cells in geologic samples with minimal physical disruption or potential for microbial contamination (Colwell et al., 1992). Petrog-

*Corresponding author. Present address: University of Illinois at Chicago, Department of Earth and Environmental Sciences, M/C 186, 845 W. Taylor St., Chicago, IL, 60607, USA.

0167-7012/99/$ – see front matter
PII: S0167-7012(99)00044-5

raphic thin sections of geologic samples retain the above contextual information.

Most previous attempts to visualize microbial biomass in geologic samples have not unequivocally identified intact cells. Nucleic acid staining has been used to detect areas with high concentrations of nucleic acids, but probably failed to identify intact microbial cells (Furnes et al., 1996; Giovannoni et al., 1996). In both recent and ancient carbonates (Folk, 1993) particles with microbial-like morphologies have been imaged with secondary electrons. Additionally, high concentrations of carbon (as determined by EDS) has been detected within reputed microfossils present in vein calcite associated with subsurface granites from Sweden (Pedersen et al., 1997).

The main goal of this study was to develop a protocol to visualize microbial cells in petrographic thin sections. An advantage of this approach is that after the cells are enumerated and morphologies noted, thin sections are amenable to electron beam analysis. Pleistocene subsurface basalts at the Idaho National Engineering and Environmental Laboratory (INEEL) were selected for this study because these samples were collected as a part of an overall investigation to determine geological controls on the composition and activity of subsurface microbial communities. Sampling and storage procedures designed to minimize microbial contamination were implemented prior to the point at which the rock chips were stained. Additionally, surface basalt samples from eastern Idaho were examined to provide material subject to more intense microbial colonization and weathering, for comparison. Two distinct fluorochromes that specifically bind to nucleic acids were utilized to visualize indigenous cells: (1) propidium iodide and (2) POPO. Both of the fluorochromes have a high affinity for double stranded DNA and RNA (Haugland, 1996); their red-to-orange emission wavelengths are distinct from the blue autofluorescence of the basalt.

In situ characterization of microbial activity using uniformly labeled ^{14}C acetate was also performed. Carboxyl labeled ^{14}C was respired as $^{14}CO_2$ whereas methyl labeled ^{14}C was incorporated into biomass (Phelps et al., 1994a,b). Unlike cell visualization with fluorochromes (total cells), measurement of ^{14}C-labeled biomass provides an indication of the distribution of viable cells.

2. Geological and microbiological setting

The eastern Snake River plain (ESRP) is a northeast trending depression located in eastern Idaho. This depression is filled mainly with volcanic constructs, which are variably covered by sedimentary deposits. Pleistocene basalt up to 2 km thick overlie older Miocene–Pliocene rhyolitic ash-flow tuffs. Pleistocene basalt consists of discrete flows formed from shield volcanism. Multiple flows that erupted nearly coevally form a flow group.

Surface basalt was collected at two outcrops in the environs of the Test Area North (TAN) site at INEEL (samples 22-1-1, 22-3-1, and 33-1-1). A third outcrop of basalt was obtained from the banks of the Snake River just upstream of the town of Idaho Falls (samples Snake-1, Snake-2). Subsurface basalt samples were collected from basaltic core from the TAN borehole 37, between 62.6 and 127.0 m (bls). The topmost core sample from this borehole occurs immediately below the water table near the P-Q sedimentary interbed. The examined interval spans the upper ESRP aquifer including basalt flow group Q to the top of the Q-R sedimentary interbeds. ESRP basalt consists of phenocrysts of olivine, plagioclase, clinopyroxene, titanomagnetite, ilmenite, and rare apatite present in a glassy groundmass. Minor alteration minerals in the basalts from this interval are associated with both vesicles and fractures and include: mainly calcite with minor calcareous Al–silicate (clay mineral?), microcrystalline silica, and pyrite (Rightmire and Lewis, 1987).

Overall, TAN-37 cores contained higher levels (than core samples from outside of the TCE plume present at TAN) of culturable microorganisms (phenol-oxidizers, propanotrophs and methanotrophs), higher levels of aerobic and anaerobic acetate mineralization and higher concentrations of extractable microbial DNA than the other area boreholes that were cored (Colwell et al., unpublished data). This is likely due to TAN-37's close proximity to the original injection well for the waste that today forms a TCE plume.

3. Methods

3.1. Sample acquisition and storage

Material from the two outcrops near TAN were collected for geologic analysis and were stored at room temperature in Zip Lock bags for 6 months before processing at room temperature under ambient light conditions. Basalt from an outcrop near Idaho Falls along the Snake River was collected moist and shipped and stored (for up to 14 days) at 4°C. All surface samples were subsampled with sterile implements into sub-centimeter sized fragments, placed into sterile 15 ml centrifuge tubes, and fixed in 4% formaldehyde. Surface samples were stored in formaldehyde at 4°C for no more than 12 h (typically 0.5 h).

Core material was collected from 62.6 to 127.0 m (bls) at TAN borehole 37 at INEEL using reverse circulation with an air/water mist. Pressurized air/water mist was introduced as drilling proceeded as a means of transporting loose rock cuttings to the surface. Water consists of ambient aquifer water disinfected with chlorine. Cores were obtained in 1.5 m segments in split barrels and immediately transported to a field laboratory, and placed into an anaerobic glovebag with an argon atmosphere for processing. For this study, samples selected in the glovebag were temporarily stored in sterile whirlpak bags. These samples were removed from the glovebag and subsampled to obtain sub-centimeter sized fragments using flame-sterilized implements. Fragments were placed into sterile 15 ml centrifuge tubes and fixed with 4% glutaraldehyde, which was added until headspace in the centrifuge tubes was eliminated. The time from sample acquisition to fixation was never greater than 3 h. Fixed samples were shipped to Princeton University and subsequently stored at 4°C until analyzed.

3.2. Nucleic acid staining procedures

Fragments of rock from a particular sample were removed from storage and placed on a sterile petri dish. Three sets of subsamples were processed: (1) stained sample; (2) heat sterilized (for a minimum of 4 h at 450°C), stained negative control; and (3) unstained sample. Additionally, selected samples from activity experiments (described below) were stained using the procedure outlined below. Subsamples were placed into sterile 15 ml centrifuge tubes. Permeabilization of cell membranes involved addition of cold (4°C) 70% v/v methanol for at least 30 min. Then samples were put into new centrifuge tubes with staining solutions of either 5 μg/ml propidium iodide (PI) or 0.1 μg/ml POPO-3 in PBS. PBS consists of NaCl (8 g/l), KCl (0.2 g/l), Na_2HPO_4 (dianhydrous, 1.44 g/l), KH_2PO_4 (0.24 g/l). The propidium iodide and POPO-3 staining solutions were made from stock solutions (50 mg/ml and 1 mg/ml, respectively) that were stored at −20°C. Staining time ranged from at least 1 h with PI to at least 1.5 h with POPO-3. Following staining the rock chips were placed into new centrifuge tubes and rinsed with 0.2 M PBS three times to assure that all the stain was removed from the sample. Samples were stored in the dark, at 4°C during staining and subsequent rinsing. All solutions were filter sterilized with a 0.22 μm pore size filter unit. After the final rinse samples were stored in the dark at 4°C until thin section preparation commenced within 1 h after rinsing was completed.

3.3. Petrographic thin section preparation

Thin sections of sub-centimeter-sized rock chips were made using no water, ultrasonic cleaners, or high temperatures (Furnes et al., 1996; Giovannoni et al., 1996); lubricating fluid used during cutting and grinding was PBS (0.2 M). Additionally, since nucleic acid stains typically fade when exposed to short wavelength visible light (<600 nm), the additional precaution of working in a darkened room illuminated by a red lamp was taken. The absorption spectra of both PI and POPO-3 decrease to near background levels at >600 nm (Haugland, 1996).

A flat surface was obtained by grinding the rock sample using a 100 fixed-grit diamond pad. This surface was further flattened with a 360 fixed-grit diamond pad. The flat surface was mounted while still slightly moist to a 25×50 mm glass slide using super glue. A cut parallel to the glass surface, was then made using a rock saw. This surface was

ground and polished using a succession of fixed-grit diamond pads (360, 600, 1500). Once completed, samples were thoroughly rinsed with PBS to remove loose rock and grit. Thin sections were stored in the dark at 4°C until direct counts were conducted. All pads were cleaned thoroughly and air dried before use to minimize the possibility of cross-contamination. The sample surface was not touched with ungloved hands and efforts were made to avoid introduction of extraneous fluorescent particles (threads, lint, and dust particles, Fig. 1b (Cercone and Pedone, 1987)).

Inefficiency of cell staining particularly for cells in small pore spaces was a concern. However, samples

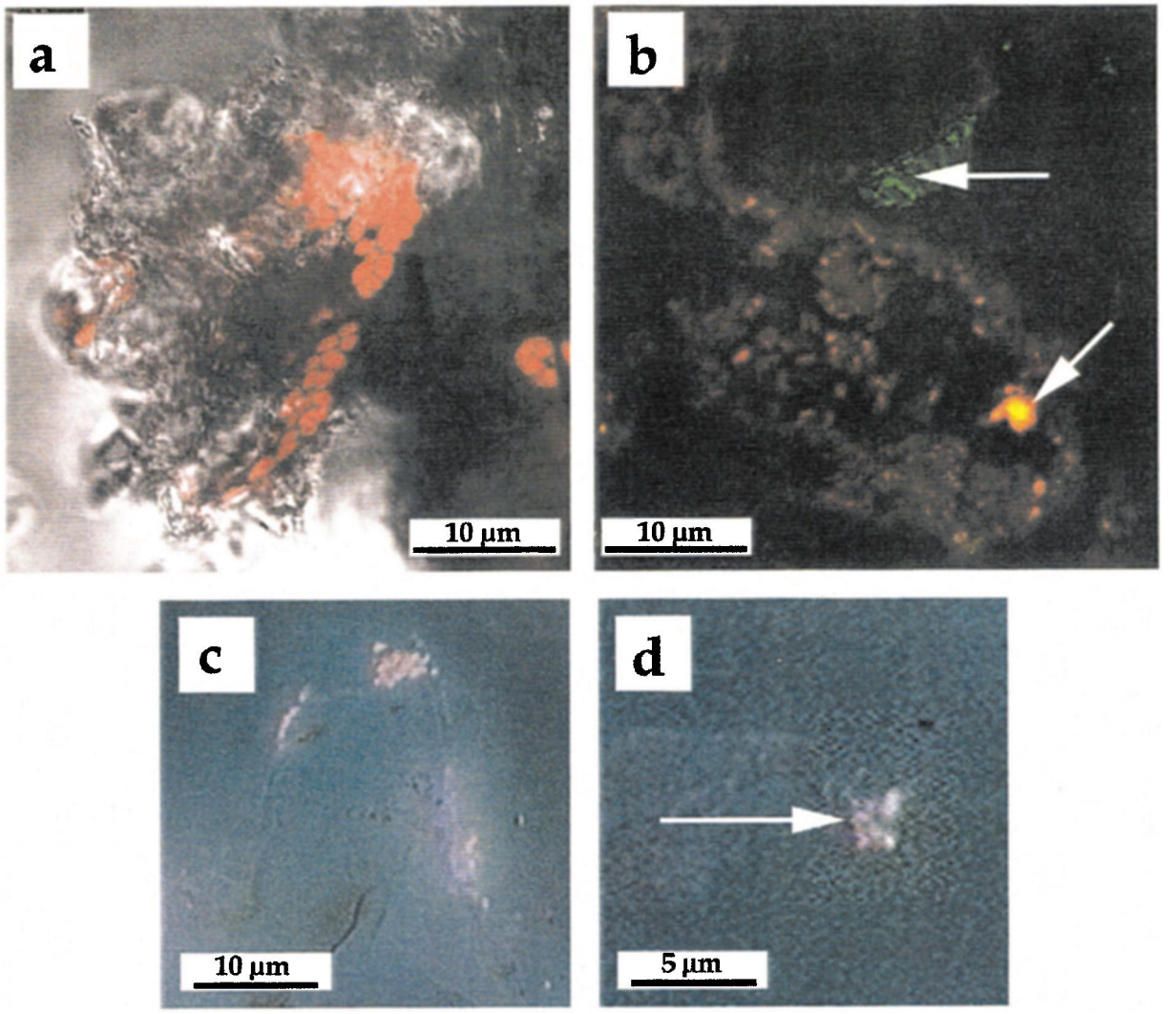

Fig. 1. Confocal (a, b) and epifluorescence (c, d) photomicrographs of PI stained cells. Epifluorescence obtained with three band filter and in which violet excitation results in background blue autofluorescence that combines with red emission from PI stained cells (observed as red with blue–green and green excitation filters) resulting in pink emission from cells. (a) PI stained diatoms (EDS indicates elevated Si) near the edge of thin section Snake-2-A. (b) PI stained bacterial rods from Snake-2-A. Arrows point to fluorescent surface contaminates. (c) Cluster of small PI stained rods from incubated subsample c. (d) Cluster of small PI rods from an unincubated subsurface sample from TAN borehole 37 (118.3 m bsl).

with large, interconnected pores were chosen and, during the initial grinding of the sample, grinding was stopped before surface-connected pores were removed. Likewise, staining time was extended by at least 30 min over that recommended for both PI (Williams et al., 1998) and POPO-3 (Matsuzaki et al., 1997).

Photobleaching is a major concern as it is accelerated by exposure to light and elevated temperature (Yu et al., 1995). The tail of the PI absorption spectra extends to greater than 600 nm and it is conceivable that exposure even to red light might cause some photobleaching. During subsequent rinsing and thin section preparation, samples were exposed cumulatively to dim red light at 20°C for no more than 1 h and at 20°C in the dark for no more than 4 h. For DAPI, a two-to-three fold decrease in the number of enumerated cells from a *Pseudomonas putida* culture has been demonstrated under the latter condition (Yu et al., 1995). This effect is probably unavoidable given that sample processing after staining takes a finite period of time and requires working with some illumination.

3.4. Microscope and filter sets

An Olympus BX-60 microscope with a 100× oil immersion objective was utilized for epifluorescence microscopy of thin sections. Non-fluorescent, Cargille type-A immersion oil was used. An accessory magnification changer facilitated visualization at total magnifications of 1000, 1250, and 1600×. Three filter sets were used to visualize microorganisms. The primary filter set (green) consisted of an excitation filter at 572±20 nm. Additional filter sets included a dual band excitation filter (blue–green) with bands between 497±17 and 571±25 nm and a three band filter (violet–blue–green) with excitation between 403±13, 496±17, and 571±26 nm. This filter set was used in conjunction with a universal cube having a three band beam splitter (average% transmission >75% between 435–475, 512–550, and 595–665 nm) and emission filter with bands at 462±1.5, 531±1.5, and 627±2 nm. Finally, some images were obtained via confocal microscopy using Zeiss LMS 510 with green excitation.

3.5. Epifluorescence microscopy of petrographic thin sections

The following three criteria were used to distinguish PI-stained fluorescent cellular material from either autofluorescing minerals or extraneous fluorescent particles introduced during sample preparation. (1) Red (or pink with violet–blue–green filter engaged) fluorescence was observed when viewed with all three filters. (2) Fluorescent particles had morphologies consistent with microbial cells. (3) Marked photobleaching occurred with prolonged excitation of several minutes. A second stain, POPO-3, was used on a surface basalt sample and independently confirmed the biogenic nature of stained fluorescent cellular material.

Images of fluorescent cells were captured using a cooled three chip color CCD camera (Optronics DEI-750; Goleta, CA, USA). These images were used to quantitatively determine photobleaching of bound stain, as a spatial guide for targeting subsequent FEG-SEM analysis (see below), and for the characterization of microbial morphometrics using Image-Pro Plus 3.0 (Media Cybernetics; Silver Spring, MD, USA).

3.6. Sample dimensions and weight

Once enumeration of fluorescent cells was completed, thin sections were scanned. The area of the thin section was determined from the scanned image. The section thickness was estimated (range 10–50 μm) from the mineral birefringence (plagioclase, olivine, pyroxene). Given these parameters, the volume of sample was determined. A bulk density was estimated to be 2.8 g/ml and the area of opaque phases in a thin section was determined by image analysis. From this information, the weight of sample examined (exclusive of opaques) by epifluorescence microscopy was determined.

3.7. Activity measurements

The purpose of this experiment was to facilitate visualization of cells in samples with known activity.

Our aim was to provide a positive control for our direct count enumeration of fixed microorganisms in geological thin sections of subsurface samples. Also, nalidixic acid inhibition of cell division was used in growth experiments to confirm the viability of visualized cells. A nominal 1 g of frozen basalt chips from TAN 37 core material were used in the activity measurements associated with this study. At the time of sample collection (June–July, 1997) this experiment was not envisioned; however, material was frozen (at $-80°C$) on the contingency that future biomarker analysis might be needed. It is the frozen material that was used in this study.

Basalt chips from four subsurface samples (TAN borehole 37) were placed in the bottom of 40 ml sterile carrier vials. The aqueous medium, which consisted of autoclaved natural groundwater from the TAN site with 0.1 μCi/ml of acetic acid–1–^{14}C or 0.2 μCi/ml of acetic acid–UL–^{14}C. This medium was made with and without nalidixic acid (5.0 mg/l) which is in the range of optimal concentrations for maximizing viable cell counts as 2.5 to 25 mg/l, indicated by Singh et al. (1989). Medium is filtered with a 0.22 μm pore size filter unit before use. Experiments were initially conducted (acetic acid–1–^{14}C) under both aerobic and anaerobic (95% N_2, 5% H_2) conditions at room temperature. However, only aerobic incubations exhibited significant activity so that in the second series (with acetic acid–UL–^{14}C) incubations were carried out only under aerobic conditions. Negative, fixed (2% v/v formaldehyde) controls were included. Once medium (up to 1 ml) was added, the sample was covered with 8 mm sterile glass beads. A sterile shell vial was perched on top of the glass beads. The shell vial contained 0.5 ml of 0.5 N NaOH. The shell vial was removed and a fresh one added three to eight times over the course of these experiments (up to 769 h). Removed shell vials were placed into larger scintillation vials to which 4 ml of OXOSOL C-14 scintillation cocktail was added. This mixture was vortexed and measured with a Pharmacia/Wallac Oy 1209 RackBeta liquid scintillation counter. At the end of the experiment, basalt chips were fixed with 2% v/v formaldehyde in which they were stored for a maximum of 72 h before implementation of the staining protocol described above.

3.8. Phosphor imaging

A Molecular Dynamics Imager System was used to analyze the distribution of ^{14}C in the thin sections made from incubated samples that exhibited significant activity. The pixel size was 88 μm for this reader and the resulting images were analyzed using Imager Quantifier Software. A thin section of the rock that did not receive any ^{14}C labeled bacteria was also included to establish a background level of radioactivity. Thin sections were exposed to the tritium screen for 168 h. The signal intensity is directly proportional to the exposure time, and hence, the activity (Dong et al., submitted). The high sensitivity of the tritium screen was achieved by removing a protective layer on the surface, allowing less energetic particles to penetrate into the plate.

3.9. FEG-SEM and EMP analysis

Samples were examined with a field emission gun scanning electron microscope (FEG-SEM) at low accelerating voltages (<7 keV) to obtain images and EDS spot analyses that corresponded to the region surrounding the cells visualized by epifluorescent microscopy and phosphor imaging. Samples were carbon coated. This work was facilitated by a low-voltage backscattered electron detector used in tandem with a large (30 mm^2) Si(Li) EDS detector to document mineral phases. Additionally, a composite backscatter image of thin section (incubated sample a) was collected with a Cameca SX-50 Electron Microprobe operating with an accelerating voltage of 25 kV and a beam current of 20 nA.

4. Results

4.1. Allometric data

Microbial cells associated with surface basalts (length = 0.3 to 3.6 μm, avg. 1.1 μm, sd = 0.5 μm) were, in general, larger than subsurface bacteria although a significant overlap in size was observed. Incubated (length = 0.2 to 1.6 μm) and non-incubated (length = 0.2 to 1.7 μm) subsurface samples exhibited nearly identical cell size distributions (for

both data sets: avg. = 0.8 μm, sd = 0.3 μm). Bacteria from all sample types exhibited both coccus and rod morphologies.

4.2. In situ cell visualization of non-incubated samples

The majority of non-incubated samples, both surface and subsurface, lacked cells (Table 1). Additionally, all negative controls and unstained samples lacked cells (Table 1) indicating that samples were not contaminated, during staining or subsequent sample preparation. Visualized cells were localized along the edges of well-connected pores; cells were not seen in internal, non-porous material. Three surface samples collected from two outcrops proximal to TAN (22-1-1, 22-3-1, 33-1-1) either did not have cells or had very few in thin section ($< 10^{3.7}$ cells/g; Table 2). Surface samples adjacent to the Snake River near Idaho Falls had variable abundance of fluorescent cells. Basalt in direct contact with the Snake River (Snake-2) had a relatively high number of PI-stained cells ($10^{5.9}$ cells/g; Table 2). Freshly broken surface basalt far from river exposure (Snake-1) had a low numbers of visualized cells similar to the TAN surface samples (Table 2). The vast majority of non-incubated subsurface samples lacked visible cells; substantially elevated biomass was evident in only one sample (116.7 to 116.8 m bsl; $10^{6.1}$ cells/g; Table 2) with three other samples having a low abundance of cells ranging from $10^{2.9}$ to $10^{4.3}$ cells/g.

Table 1
Samples examined

	Total number of samples	Number of samples with one or more cells
Surface Samples	24	9
Negative Controls	9	0
Subsurface Samples	36	7
Unincubated Samples	32	4
Incubated Samples	4	3
Negative Controls	8	0
Surface Samples		
22-1-1 (n = 6)		
22-3-1 (n = 6)		
33-1-1 (n = 2)		
Snake-1 (n = 6)		
Snake-2 (n = 2)		
Subsurface Samples		
Incubated Samples		
TAN well 37 - 116.7 to 116.8 m bsl (n = 4)		
Unincubated Samples - TAN well 37		
68.0 m bsl (n = 4)		
73.4 to 73.5 m bsl (n = 2)		
76.4 to 76.5 m bsl (n = 2)		
77.2 m bsl (n = 3)		
78.5 m bsl (n = 2)		
96.9 to 97.0 m bsl (n = 4)		
113.2 to 113.3 m bsl (n = 1)		
115.7 to 115.8 m bsl (n = 2)		
116.7 to 116.8 m bsl (n = 2)		
118.3 m bsl (n = 3)		
119.9 to 120.0 m bsl (n = 2)		
122.0 to 122.1 m bsl (n = 2)		

4.3. Activity measurements and in situ cell visualization of incubated samples

Many incubated subsurface samples (including all fixed controls) did not exhibit significant activity over the course of the experiment. No significant activity was recorded in anaerobic samples (data not shown). Some aerobic samples both with and without nalidixic acid yielded activity (Fig. 2). However, even in samples with significant activity, acetate mineralization rates (1 to 4 pm/g/day; Fig. 2) were significantly lower than previously measured on fresh material from TAN 37, which was 202.8 pm/g/day (Fig. 2). The fact that this sample was frozen for 8 to 11 months at −80°C prior to incubation likely was responsible for the lower activities measured in this study, since the prevalent effect of prolonged freezing on cells is lysis of the cell walls (Vorobyova et al., 1997; Soina et al., 1996).

Thin sections of fixed basalt chips were made following incubations with acetic acid–UL–^{14}C. Subsequently, these thin sections were placed in a phosphor imager to analyze the distribution of ^{14}C incorporated into biomass during the incubation experiment. Two subsamples with significant ^{14}C incorporation into biomass also had a high degree of ^{14}C acetate mineralization to $^{14}CO_2$ (samples a and c; Figs. 2b and 3). A high abundance of PI-stained

Table 2
Number of cells determined by PI staining and estimated biomass (only samples with cells are shown)

Sample	Subsample	Number of Cells	Area of rock (cm^2) corrected for opaques	Weight of volume (mg) examined	Number of cells $\log_{10}$cells g^{-1}
Surface samples					
22-1-1	a	1	0.0748	1.05	3.0
22-1-1	b	0	0.1386	1.93	<2.7
22-1-1	c	0	0.3498	4.90	<2.3
22-1-1	d	0	0.0674	0.94	<3.0
22-1-1	e	0	0.0772	1.08	<3.0
22-1-1	f	0	0.0154	0.22	<3.7
22-3-1	a	4	0.1842	2.58	3.2
22-3-1	b	4	0.1823	1.79	3.4
22-3-1	c	9	0.1352	1.89	3.7
22-3-1	d	0	0.1493	2.09	<2.7
22-3-1	e	0	0.0767	1.07	<3.0
22-3-1	f	0	0.0967	1.35	<2.9
Snake - 1	a	1	0.1922	2.69	2.6
Snake - 1	b	0	0.2107	2.94	<2.5
Snake - 1	c	0	0.1645	1.15	<2.9
Snake - 1	d	0	0.1183	1.66	<2.8
Snake - 1	e	0	0.0137	0.19	<3.7
Snake - 1	f	0	0.0890	1.25	<2.9
Snake - 2	a	566	0.0431	0.63	5.9
Snake - 2	b, c, &d	*			
Incubated subsurface samples					
116.7 to 116.8 mbls					
	a	*			
	b	0	0.0961	0.81	0.81
	c	92	0.0009	0.01	0.01
	d	12	0.1965	2.75	2.75
Unincubated subsurface samples					
116.7 to 116.8 mbsl	a	44	0.0024	0.03	6.1
	b	0	0.1069	0.90	<3.0
118.3 mbsl	a	7	0.0248	0.34	4.3
	b	0	0.3799	3.19	<2.5
	c	0	0.4828	6.76	<2.2
119.9 to 120.0 mbsl	a	2	0.1752	2.45	2.9
	b	0	0.0471	0.13	<3.9
122.0 to 122.1 mbsl	a	4	0.2165	2.72	3.2
	b	0	0.2752	3.85	<2.4

* Cells observed but not enumerated.

cells ($10^{6.9}$ cells/g; Table 2) was also visualized in these samples (Table 2, Fig. 3). Interestingly, in the thin section of a third subsample with elevated ^{14}C acetate mineralization to $^{14}CO_2$, the observed incorporation of ^{14}C into biomass was minimal (sample b; Figs. 2b and 3). Additionally, no PI-stained cells were visualized in this thin section indicating a biomass of $<10^{3.1}$ cells/g (Table 2). Finally, a fourth subsample with limited ^{14}C acetate mineralization to $^{14}CO_2$ also exhibited little ^{14}C labeled biomass in thin section (sample d; Figs. 2b and 3), but some PI-stained cells where visualized ($10^{3.6}$ cells/g; Table 2, Fig. 3).

A significant edge effect exists with a considerable amount of activity concentrated at the edges of samples a and c. This could be an artifact of the incubation because ^{14}C acetate was added to the surface of the sample. Therefore, it is at these sites

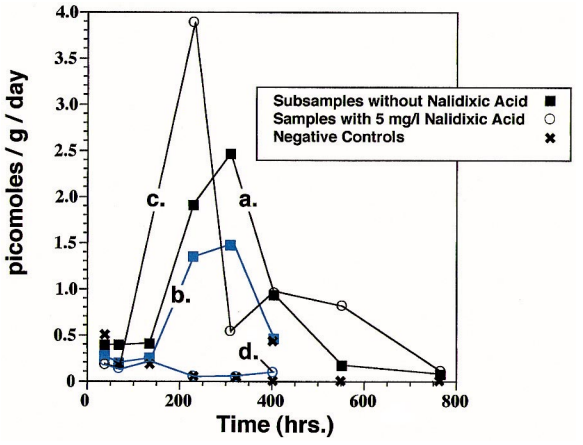

Fig. 2. Incubation experiments (acetic acid–UL–^{14}C) from TAN borehole 37, sample from 116.7 to 116.8 m bls (a, b, c, and d refer to corresponding subsample shown in Fig. 3).

that one might expect a greater concentration of ^{14}C labeled biomass. Therefore, it is suggested that in future studies that intact samples be incubated and subsequent thin sections be made of the interior of the incubated sample to avoid this edge effect.

4.4. Relationship of visualized cells with mineralogy and texture

The most basic relationship between PI visualized cells and mineralogy is artifactual with cells confined to translucent phases (phenocrysts of plagioclase, pyroxene, olivine). Note that biomass estimates in Table 2 are corrected for opaque areas and consider only translucent areas of the thin section. However, some cells were associated with partially oxidized, Fe-rich silicates that are semi-opaque. When the phosphor image of incubated sample a (Fig. 3a) is compared with backscatter images from this sample (Fig. 4) the distribution of viable cells within the sample do not seem to have a specific mineralogical preference; however, the relative coarse spatial resolution of the phosphor image makes this conclusion equivocal. More significantly, within the incubated samples a and c cells, with incorporated ^{14}C, are confined to large, well-connected pores (Figs. 3 and 4). Cells are absent from the more massive areas within the basalt that lack well-connected porosity.

5. Discussion and summary

PI staining and phosphor imaging allowed for the visualization of microbial cells in thin sections of geological material. However, the lack of proper storage makes an interpretation of the TAN surface basalts difficult. Storage of the surface basalts collected from the environs of the Snake River is less problematic. Snake-1 (a basalt not in direct contact with the Snake River) exhibited a low biomass like TAN surface basalts with no biological ‘hot spots’ visualized in six examined subsamples (Table 2). Conversely, cells were visualized in all the subsamples examined of the sample Snake-2 (a basalt in contact with the Snake River, Table 2).

In contrast to surface samples, subsurface basalts exhibited a significant degree of intrasample heterogeneity in the distribution of bacteria. This heterogeneity in microbial biomass was best illustrated by the non-incubated and incubated (with acetic acid–UL–^{14}C) samples from 116.7 to 116.8 m bls. Two non-incubated subsamples were examined from this level. No cells were visualized in one (non-incubated sample 116.7 to 116.8 m bls, b; Table 2); whereas, bacterial cells were commonly detected in the other as determined by PI staining (non-incubated sample 116.7 to 116.8 m bls, a; Table 2). The heterogeneity of incubated samples from this stratigraphic level is demonstrated by PI staining, acetate mineralization to $^{14}CO_2$ measurements, and phosphor imaging of ^{14}C incorporated into bacterial cells. PI staining revealed that cells were present in three out of four incubated subsamples (a, c and d). Additionally, significant acetate mineralization was observed in three subsamples (a, b and c); whereas, biomass with incorporated ^{14}C was detected in only two subsamples (a and c). Negative measurements of metabolic potential are common in incubations with lithic material, particularly if sample size is small, <10 g (Stevens and Holbert, 1995). Therefore, the lack of activity in some of the subsamples is not surprising and is an indication of the centimeter-scale heterogeneity of biomass distribution characteristic of subsurface terrestrial environments (Brockman and Murray, 1997).

Additionally, the inconsistencies of the biomass determinations for incubated samples b and d are significant (Table 2; Fig. 3). Subsample d exhibited

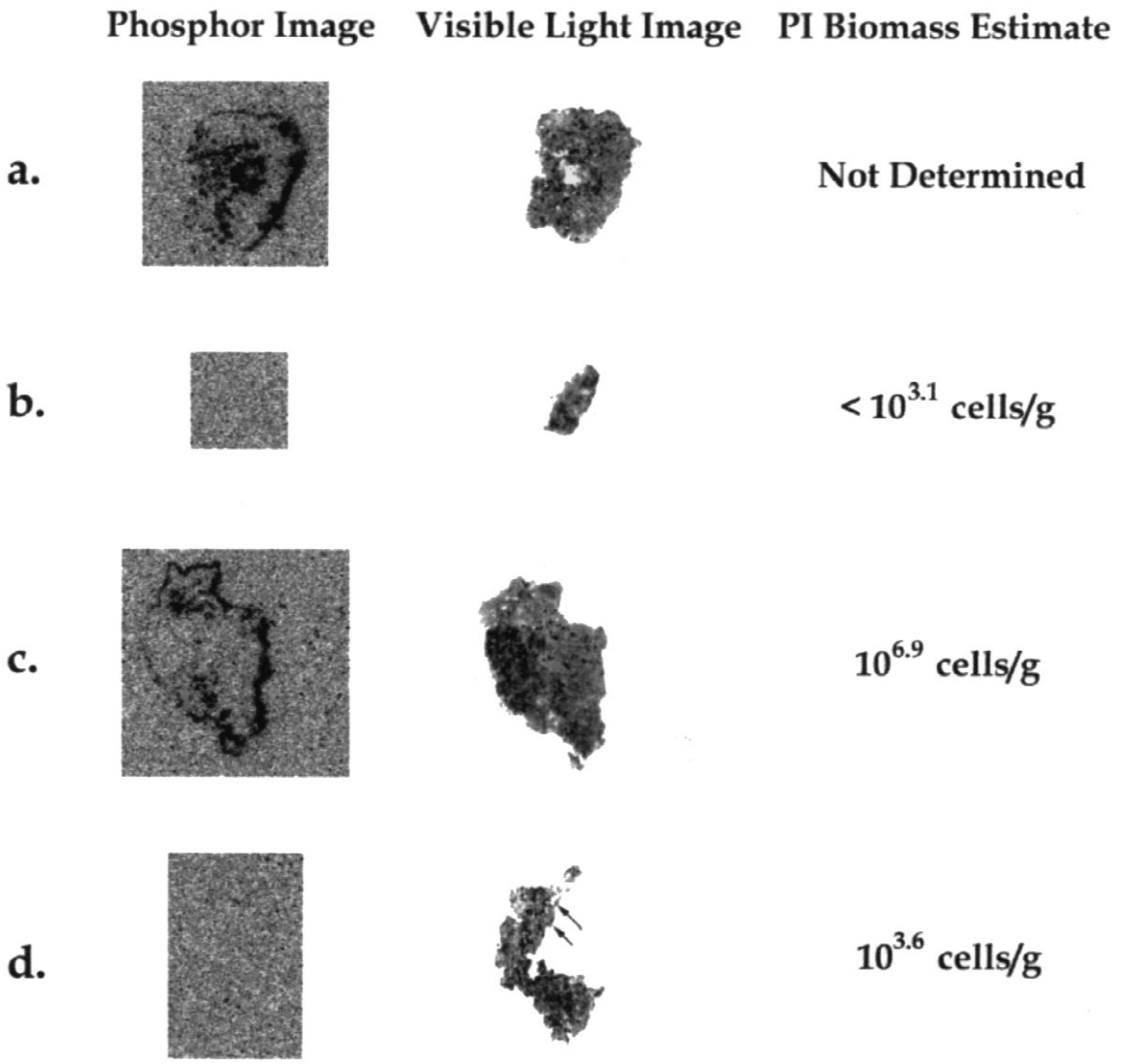

Fig. 3. The ^{14}C distribution (as measured by phosphor imaging) in four thin sections of basalt chips from 116.7 to 116.8 m (bsl) at TAN borehole 37 that were aerobically incubated with acetic acid–UL–^{14}C paired with visible light image of the corresponding thin section. Note that the images are at a 1:1 scale. The number of PI-enumerated cells in each sample is indicated. Arrows in d point to the two areas where cells were visualized with PI staining.

insignificant acetate mineralization into $^{14}CO_2$ along with nondetectable ^{14}C biomass as determined by phosphor imaging. However, 12 cells were visualized by PI staining (Fig. 3). Therefore, these cells probably did not incorporate ^{14}C labeled biomass; PI visualized cells are close to the surface of the sample therefore shielding of labeled biomass is not considered likely.

In subsample b cells were not visualized by either PI staining or phosphor imaging. However, significant acetate mineralization was measured from this subsample (Fig. 2). The mass examined in the thin section of subsample b was 1.21 mg (Table 2) versus a total mass of the sample used in the incubation experiment of 1.81 g. Therefore, significant biological activity was not present in the 0.07% of the

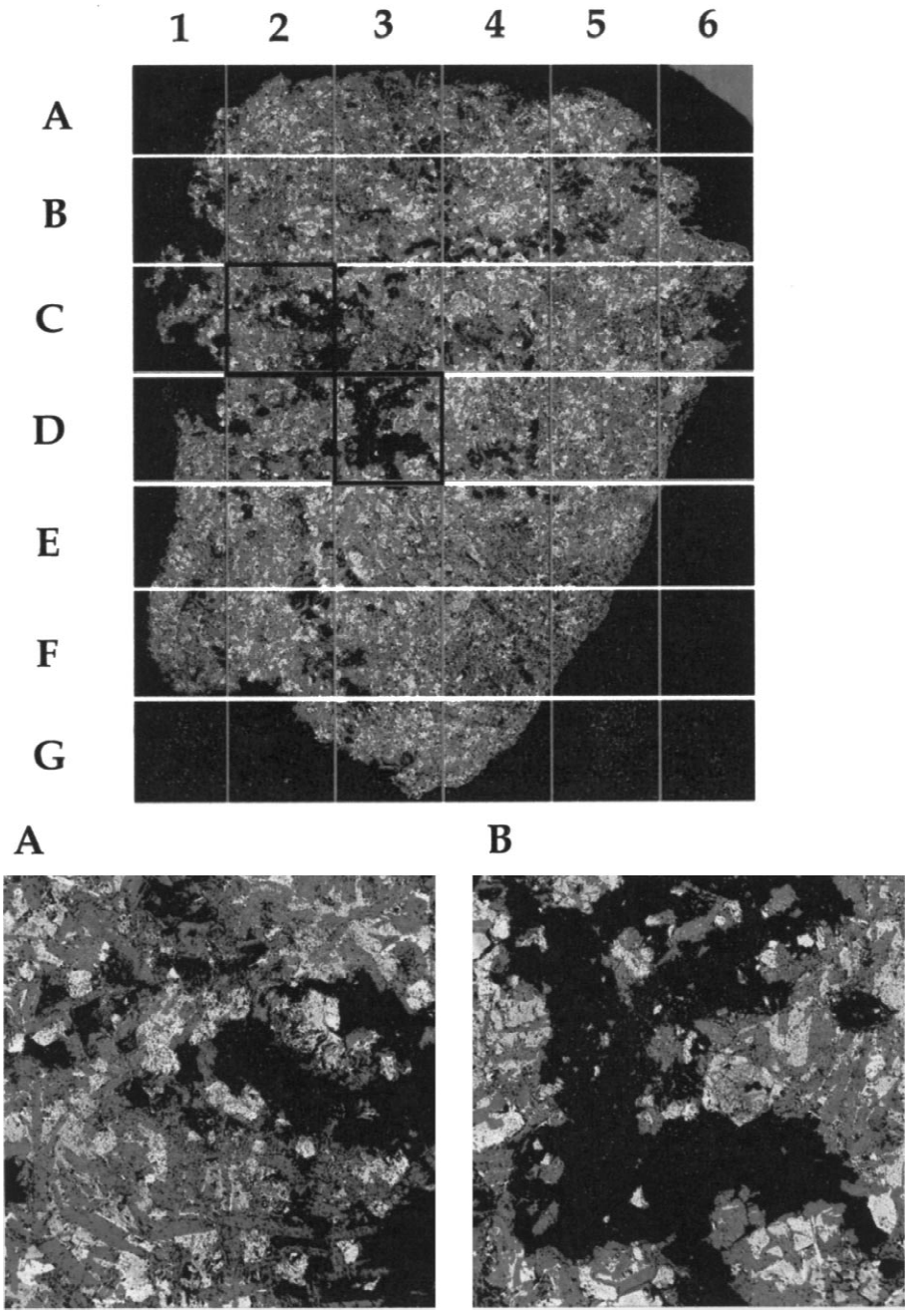

Fig. 4. Backscatter electron image of incubated sample a from 116.7 to 116.8 m (bsl). Average atomic number (Z) of material is indicated (low Z dark; high Z bright). For example Fe-rich phases such as olivine and Fe-oxides are white whereas plagioclase is dark gray. Note that porosity, which is filled with a carbon-rich epoxy, shows up as black. Image has a scale of 8:1. Blow-ups A and B are backscatter images the come from grids C2 and D3, respectively.

sample examined and CO_2 mineralization must be associated with biological activity that occurred elsewhere in this subsample; a demonstration of sub-centimeter-scale heterogeneity. Indeed sub-centimeter-scale heterogeneity is directly observed in subsamples a and c (Figs. 3 and 4). These samples are larger and have well-connected porosity. Given the lack of large pores present in subsample b it should not be surprising that this subsample lacks biomass.

In conclusion, we have developed two methods in which one can visualize cells in petrographic thin sections. These methods can be applied to other lithologies. The main constraint is that well-connected porosity must exist to allow the advection of reagents into and out of the sample. The fundamental realization one needs to make when applying this method is that cells in small, poorly connected pores will be under-represented. Therefore, ideal results will be achieved in lithologies with relatively large and uniform sized pores. An example of this type of lithology includes sands (Dong et al., submitted) and poorly consolidated sandstones. Highly biased results (biased toward visualizing cells in large, well-connected openings) is expected in fractured crystalline rock (e.g. limestone, granite).

Acknowledgements

This research is supported by a grant from the Environmental Science Management Program DE-AC07-76IDO1570 from the Department of Energy (DOE) to F.S. Colwell with additional support from DOE grant DE-FG02-94ER61821 to T.C.O. The authors are grateful for the assistance rendered by M. Fuller, K. Gillespie, S. Streger, P. Hatzinger of Envirogen, Inc. of Lawerenceville, NJ and E. Vicenzi at the Princeton Material Institute.

References

Cercone, K.R., Pedone, V.A., 1987. Flourescence (photoluminescence) of carbonate rocks: instrumental and analytical sources of observational error. J. Sedimentary Petrol. 57, 780–782.

Colwell, F.S., Stormberg, G.J., Phelps, T.J., Birnbaum, S.A., McKinley, J., Rawson, S.A., Veverka, C., Goodwin, S., Long, P.E., Russell, B.F., Garland, T., Thompson, D., Skinner, P., Glover, S., 1992. Innovative techniques for collection of saturated and unsaturated subsurface basalts and sediments for microbiological characterization. J. Microbial Methods 15, 279–282.

Folk, R.L., 1993. SEM imaging of bacteria and nannobacteria in carbonate sediments and rocks. J. Sedimentary Petrol. 62, 990–999.

Haugland, R.P. (1996) Handbook of Fluorescent Probes and Research Chemicals. 679 pp. Molecular Probes. Eugene, OR, USA.

Hiebert, F.K., Bennett, P.C., 1992. Microbial control of silicate weathering in organic-rich ground water. Science 258, 278–281.

Kepner, R.L., Pratt, J.R., 1993. Effects of sediments on estimates of bacterial density. Trans. Am. Microscop. Soc. 112, 316–330.

Lovley, D.R., Chapelle, F.H., Phillips, E.J.P., 1990. Fe(III)-reducing bacteria in deeply buried sediments of the Atlantic Coastal Plain. Geology 18, 954–957.

Matsuzaki, T., Suzuki, T., Fujikura, K., Takata, K., 1997. Nuclear staining for laser confocal microscopy. Acta Histochem. Cytochem. 30, 309–314.

Pedersen, K., Ekendahl, S., Tullborg, E.-L., Furnes, H., Thorseth, I., Tumyr, O., 1997. Evidence of ancient life at 207 m depth in a granitic aquifer. Geology 25, 827–830.

Phelps, T.J., Murphy, E.M., Pfiffner, S.M., White, D.C., 1994a. Comparison between geochemical and biological estimates of subsurface microbial activities. Microbial Ecol. 28, 335–349.

Phelps, T.J., Pfiffner, S.M., Sargent, K.A., White, D.C., 1994b. Factors influencing the abundance and metabolic capacities of microorganisms in eastern coastal plain sediments. Microbial Ecol. 28, 351–364.

Singh, A., Pyle, B.H., McFeters, G.A., 1989. Rapid enumeration of viable bacteria by image analysis. J. Microbiol. Methods 10, 91–101.

Soina, V.S., Vorobiobiova, E.A., Zvyagintsev, D.G., Gilichinsky, D.A., 1996. Preservation of cell structures in permafrost: a model for exobiology. Adv. Space Res. 15, 237–242.

Stevens, T.O., McKinley, J.P., 1995. Geochemically produced hydrogen supports microbial ecosystems in deep basalt aquifers. Science 270, 450–454.

Stevens, T.O., Holbert, B.S., 1995. Variability and density dependence of bacteria in terrestrial subsurface samples: implications for enumeration. J. Microbial Methods 21, 283–292.

Vorobyova, E., Soina, V., Gorlenko, M., Minkovskaya, N., Zalinova, N., Mamukelashvili, A., Gilichinsky, D., Rivkina, E., Vishnivetskaya, T., 1997. The deep cold biosphere: facts and hypothesis. FEMS Microbiol. Rev. 20, 261–276.

Williams, S.C., Hong, Y., Danavall, D.C.A., Howard-Jones, M.H., Gibson, D., Frischer, M.E., Verity, P.G., 1998. Distinguishing between living and nonliving bacteria: evaluation of the vital stain propidium iodide and the combined use with molecular probes in aquatic samples. J. Microbiol. Methods 32, 225–236.

Yu, W., Dodds, W.K., Banks, K., Skalsky, J., Strauss, E.A., 1995. Optimal staining and sample storage time for direct microscopic enumeration of total and active bacteria in soil with two fluorescent dyes. Appl. Environ. Microbiol. 61, 3367–3370.

Rightmire, C.T., Lewis, B.D., 1987. Hydrogeology and geochemistry of the unsaturated zone, Radioactive Waste Management Complex, Idaho National Engineering Laboratory, Idaho. USGS Water-Resources Investigations Report 87–4198. US Geological Survey, Idaho, p. 90.

Dong, H., Onstott, T.C., MeFlaun, M.F., Fuller, M., Gillespie, K., Fredrickson, J.K. Development of radiographic and microscopic techniques for the characterization of bacterial transport in intact sediment cores from Oyster, Virginia, submitted.

Brockman, F.J., Murray, C.J., 1997. Microbiological heterogeneity in the terrestrial subsurface and approaches for its description. In: Amy, P.S., Haldeman, D.L. (Eds.), The Microbiology of the Terrestrial Deep Subsurface, pp. 74–104.

Furnes, H., Thorseth, I.H., Tumyr, O., Torsvik, T., Fisk, M.R., 1996. Microbial activity in the alteration of glass from pillow lavas from Hole 896A. Proceedings of the Ocean Drilling Program, Scientific Results. 148, 191–206.

Giovannoni, S.J., Fisk, M.R., Mullins, T.D., Furnes, H., 1996. Genetic evidence for endolithic microbial life colonizing basaltic glass/seawater interfaces. Proceedings of the Ocean Drilling Program, Scientific Results. 148. Ocean Drilling Program, Texas, pp. 207–214.